The American Journal of Pathology, Vol. 173, No. 2, August 2008

DOI: 10.2353/ajpath.2008.071208

Neurobiology

Dynamin-Like Protein 1 Reduction Underlies Mitochondrial Morphology and Distribution Abnormalities in Fibroblasts from Sporadic Alzheimer's Disease Patients

Xinglong Wang,* Bo Su,* Hisashi Fujioka,† and Xiongwei Zhu*

From the Departments of Pathology and Pharmacology,† Case Western Reserve University, Cleveland, Ohio*

Mitochondrial function relies heavily on its morphology and distribution, alterations of which have been increasingly implicated in neurodegenerative diseases, such as Alzheimer's disease (AD). In this study, we found abnormal mitochondrial distribution characterized by elongated mitochondria that accumulated in perinuclear areas in 19.3% of sporadic AD (sAD) fibroblasts, which was in marked contrast to their normally even cytoplasmic distribution in the majority of human fibroblasts from normal subjects (>95%). Interestingly, levels of dynamin-like protein 1 (DLP1), a regulator of mitochondrial fission and distribution, were decreased significantly in sAD fibroblasts. To explore the potential role of DLP1 in mediating mitochondrial abnormalities in sAD fibroblasts, both the overexpression of a dominant negative DLP1 mutant and the reduced expression of DLP1 by miR RNAi in human fibroblasts from normal subjects significantly increased mitochondrial abnormalities. Moreover, overexpression of wild-type DLP1 in sAD fibroblasts rescued these mitochondrial abnormalities. Based on these data, we conclude that DLP1 reduction causes mitochondrial abnormalities in sAD fibroblasts. We further demonstrate that elevated oxidative stress and increased amyloid β production are likely the potential pathogenic factors that cause DLP1 reduction and abnormal mitochondrial distribution in AD cells. ***(Am J Pathol 2008, 173:470–482; DOI: 10.2353/ajpath.2008.071208)***

Alzheimer's disease (AD) is the leading cause of dementia in the elderly, characterized by neurofibrillary tangles, senile plaques, and progressive loss of neuronal cells in selective brain regions.[1] Whereas there are a myriad of striking alterations in the diseased brain, the pathogenesis of the disease is still currently poorly understood. Among these changes, oxidative stress is one of the earliest and may play a critical role in the disease.[2] Mitochondria can be both targets of oxidative damage and sources of reactive oxygen species (ROS), and mitochondrial damage occurs during the aging process,[3] which is associated with memory loss.[4] In fact, damaged mitochondria are less efficient producers of ATP and more efficient producers of ROS. In AD, metabolic abnormalities[5] as well as damage to both the components and the structure of mitochondria are evident.[6–8] Interestingly, quantitative morphometric studies not only confirm that neurons in AD demonstrate a higher percentage of damaged mitochondria but also reveal enlarged mitochondrial size with decreased mitochondria number in AD neurons.[2,9] The latter finding suggests that the normally strict regulation of mitochondria morphology is impaired, an assertion supported by work showing that AD cybrid cells also contain a significantly increased percentage of enlarged mitochondria.[10]

Mitochondrial morphology is dynamic and controlled by continual and balanced fission and fusion events that are regulated by a machinery involving large dynamin-related GTPases that exert opposing effects, eg, dynamin-like protein 1 (DLP1, also referred to as Drp1, DVLP, dymple, HdynIV and DNM1P)[11–15] for fission, and optic atrophy 1 (OPA1) for fusion.[16] By regulating mitochondrial fission/fusion, DLP1 and fusion protein control the morphology and distribution of mitochondria.[17] Nor-

Supported by National Institutes of Health grant AG031852 and Alzheimer's Association grant IIRG-07-60196.

Accepted for publication April 22, 2008.

Supplemental material for this article can be found on *http://ajp.amjpathol.org*.

Address reprint requests to Xiongwei Zhu, Ph.D., Department of Pathology, Case Western Reserve University, 2103 Cornell Road, Cleveland, OH 44106. E-mail: xiongwei.zhu@case.edu.

mal mitochondrial fission is critical to meet the energy demands of cells at particular subcellular locations, which is of special importance for extremely polarized cells such as neurons,[18] whose synaptic terminals have abundant mitochondria.[19] Of that, impairments in the balance of mitochondria fission and fusion are being increasingly implicated in neurodegenerative diseases. For example, Charcot-Marie-Tooth neuropathy type 2A is caused by mutations in Mfn2,[20,21] and the most commonly inherited optic neuropathy is caused by mutations in OPA1, another protein involved in mitochondrial fusion.[22,23] However, few studies to date have examined mitochondrial dynamics in AD.

Fibroblasts are valuable tools to study mitochondrial abnormalities during aging[24] and relate to AD, since various parameters of altered energy metabolism have been reported including increased lactate production and altered glucose utilization as well as defects in various mitochondrial enzymes.[25–29] In this study, we found profound alterations in mitochondria morphology and distribution in human fibroblasts from sporadic Alzheimer's disease (sAD) patients compared to normal subjects. To understand the underlying mechanisms of such mitochondria alterations in sAD fibroblasts, we either overexpressed or knocked down functional DLP1 in fibroblasts and examined the effects of these manipulations. We further determined the effect of oxidative stress and overexpression of amyloid β protein precursor (APP) or Swedish mutant APP on DLP1 levels and mitochondrial alterations. Our findings implicate alterations in mitochondrial fission/fusion as an underlying mechanism of the mitochondrial dysfunction in AD.

Materials and Methods

Cell Lines, Cell Culture, and Transfection

Fibroblasts from nine age-matched normal (age 69 $\pm$ 9 years; sex, M:F = 5:4) and nine patients with sAD (age 71 $\pm$ 9 years; sex, 5:3 and one patient without information about sex) were obtained from Coriell Institute for Medical Research with a similar cumulative population doubling level (CPDL) of 11.1 $\pm$ 3.3. CPDL reflected relative age of cells in culture. All of the AD patients were clinically diagnosed and six of them were confirmed at autopsy. No pathology information was available for the remaining AD cases and control cases. Depending on its CPDL, these cells were additionally passed several times to match their CPDL[16–18] before any experiment was performed. Cells plated on flask or chamber slides coated with fibronectin (BD, San Jose, CA) were grown in minimum essential medium (Invitrogen, Carlsbad, CA) containing nonessential amino acids and 2 mmol/L glutamine, supplemented with 10% or 15% (v/v) fetal bovine serum, in 5% CO_2 in a humid incubator at 37°C. Cells were transfected using the FuGENE HD (Roche, Indianapolis, IN) or Effectene (QIAGEN, Valencia, CA) according to the manufacturers' instructions. For cotransfection, 3:1 ratio (indicated plasmid: mito-DsRed2) was applied.

Expression Vectors and Antibodies

Mito-DsRed2 construct (Clontech, Mountain View, CA), expression plasmids for HA tagged-DLP1 and HA tagged-DLP1 K38A (from Dr. Yisang Yoon, University of Rochester), wild-type (WT) APP and Swedish mutant APP (APPswe) (from Dr. Huaxi Xu, The Burnham Institute), and dominant negative mutant BACE1 D92T (from Dr. Riqiang Yan, Lerner Research Institute) were obtained. DLP1 miR RNAi vector was generated via pcDNA 6.2-GW/EmGFP-miR construct (Invitrogen). We designed the 21-mer miR RNAi sequence (5′-AACCCTTCCCATCAATACATC-3′) targeting the open reading frame region of human DLP1 (BLOCK-iT RNAi Designer, Invitrogen). Primary antibodies used included mouse anti-DLP1 (BD), mouse anti-APP (4G8, Covance, Denver, CO) and anti-α-tubulin and HA (Cell Signaling, Danvers, MA).

Cell Treatments and Measurements

Fibroblasts grown to 60 to 80% confluence were treated with 50 μmol/L H_2O_2 in normal growth media for 1 hour. Cells were rinsed at least two times with fresh media and incubated at 37°C in fresh media for an additional 3 hours and examined. Vitamin E (Sigma, St. Louis, MO) was added separately to the medium 1 hour before, during, and after the H_2O_2 treatment. H_2O_2 cytotoxicity was measured by cytotoxicity detection kit (LDH; Roche) as previously described.[7] To measure ROS, fluorescent probe carboxydichlorodihydrofluorescein diacetate (DCF, Invitrogen) was used according to the manufacturer's instruction. To induce heme deficiency, fibroblasts were treated with 10 μmol/L *N*-methylprotoporphyrin IX for 6 days as previously described.[30] One day before drug treatment, fibroblasts were transfected with mito-DsRed2 to specifically marking mitochondria. Mitochondrial membrane potential was measured by red/green fluorescence ratio of 5,5′,6,6′-tetrachloro-1,1′,3,3′-tetraethylbenzimidazolocarbocyanine (JC-1, Invitrogen). Senescence-associated β-galactosidase was assayed by cellular senescence assay kit per the manufacturer's instructions (Millipore, Billerica, MA).

Western Blot Analysis

Cells were lysed by cell lysis buffer (Cell Signaling) plus 1 mmol/L phenylmethylsulfonyl fluoride (Sigma) and protease inhibitor cocktail (Sigma). Equal amounts of total protein extract (20 or 50 μg) were resolved by sodium dodecyl sulfate-polyacrylamide gel electrophoresis and transferred to Immobilon (Millipore). After blocking with 10% nonfat dry milk, primary and secondary antibodies were applied as previously described[7] and the blots developed with Western blotting luminol reagent (Santa Cruz, Santa Cruz, CA).

Flow Cytometric Analysis and Fibroblast Synchronization

To determine the cell cycle phase distribution of normal human fibroblasts (NHFs) and sAD fibroblasts, flow cyto-

metric analysis was performed as previously reported.[31] Experiments were repeated three times for each sample. To synchronize fibroblasts, cells were seeded at a concentration of 2×10^4 cells/cm^2 in a 75-ml flask and grown to 60 to 80% confluence to obtain exponentially growing cells. For serum starvation experiments, cultures were washed three times with serum-free minimum essential medium and then cultured in minimum essential medium with only 0.2% fetal bovine serum for 18 hours.[32] For chemical synchronization, cultures were incubated with regular minimum essential medium culture media containing 0.5 mmol/L hydroxyurea for 18 hours and then released into drug-free medium.[33] Synchronization was confirmed by staining fibroblasts with propridium iodide/RNase staining buffer (BD) 24 hours or 72 hours after serum addition or drug removal, which was examined by confocal microscopy.[34] To measure mitochondria distribution in synchronized fibroblasts, fibroblasts were plated on chamber slides after serum starvation or drug treatment for 24 hours in regular minimum essential medium supplemented with 10% fetal bovine serum and then transfected with mito-DsRed2. 48 hours after transfection, cells were fixed, immunostained, and examined as described below. At least 1000 cells for each condition were measured. Experiments were repeated twice.

Electron Microscopy

Human fibroblast cells (three lines of NHFs and three lines of sAD fibroblasts) were cultured on the Aclar embedding film (2 mil thickness, Electron Microscopy Sciences, Hatfield, PA), fixed in 2.0% glutaraldehyde and 4% sucrose in a 0.05 mol/L phosphate buffer, pH 7.4, for 2 hours and then postfixed in 1% osmium tetroxide for 1 hour. Samples were then block-stained in 0.5% aqueous uranyl acetate, dehydrated, and embedded in Epon 812. Ultrathin sections (three sections/sample) stained with 2% uranyl acetate in 50% methanol and lead citrate were examined in a Zeiss CEM902 electron microscope (Oberkochen, Germany). Each ultrathin section contained 20 to 30 cells.

Immunofluorescence

Fibroblasts were cultured on chamber slides coated with fibronectin (BD). After treatment, cells were washed twice with prewarmed phosphate-buffered saline and then fixed with 4% paraformaldehyde for 45 minutes at room temperature. Cells were permeabilized with 0.5% Triton X-100 for 30 minutes, blocked with 10% normal goat serum for 30 minutes, and incubated with primary antibodies in phosphate-buffered saline containing 1% normal goat serum overnight at 4°C. After three washes with phosphate-buffered saline, cells were incubated in 10% normal goat serum for 10 minutes and then with Alexa Fluor 488/647-conjugated secondary antibody (Invitrogen) (1:300) for 1 hour at 37°C in the dark. Cells were rinsed three times with phosphate-buffered saline and mounted with antifade medium (Southern Biotech, Birmingham, AL). All fluorescence images were captured with a Zeiss LSM 510 inverted fluorescence microscope or a Zeiss LSM 510 inverted laser-scanning confocal fluorescence microscope (Zeiss, Oberkochen, Germany). Confocal images of Pc 4 fluorescence were collected using 633-nm excitation light from a HeNe laser and a 650-nm long-pass filter. Images of mito-DsRed2 red fluorescence were collected using 543-nm excitation light from an argon laser and a 560-nm long-pass filter. Green fluorescence was collected using 488-nm excitation light from an argon laser and a 500- to 550-nm bandpass barrier filter. Image analysis was performed with open-source image analysis programs WCIF ImageJ (developed by W. Rasband) and Image-Pro Plus 6.0 (Media Cybernetics, Bethesda, MD).

For quantification of abnormal mitochondrial distribution, at least 1000 cells were measured for each cell line. In each cell, the perinuclear area was defined as the area encircling the nucleus having a radius twofold the length of the longer arm of the nucleus. The amount, or intensity, of MitoDs-Red2 signal was measured both within this perinuclear area as well as within the entire cell. The ratio of these two values was calculated, giving the percentage of mitochondria within the perinuclear area (see Supplemental Figure S1 at *http://ajp.amjpathol.org*). The cell was classified as having a partially collapsed mitochondria network if at least 60% of the mitochondria were present in the perinuclear area. If more than 95% of mitochondria are present in the perinuclear area, the cell was classified with complete mitochondrial network collapse.

For quantification of DLP1 levels, high-magnification pictures of fibroblasts were analyzed by Image-Pro Plus 6.0 (Media Cybernetics) to separate positive and negative immunolabeling and to calculate the value of intensity of DLP1 immunofluorescence labeling within each individual cell. The background fluorescence intensity was determined and subtracted from values obtained. DLP1 level of a given fibroblast was determined by relative total immunofluorescence labeling of DLP1 (total immunofluorescence intensity of DLP1/total area of the fibroblast). To eliminate the variance of slides, we defined the relative mean value of DLP1 level in fibroblasts with normal mitochondrial network as 1. Each experiment was repeated at least three times.

Results

Mitochondrial Morphology and Distribution Change in sAD Fibroblasts

Previous studies have demonstrated abnormal changes in mitochondrial morphology in AD neurons.[9] In this study, we sought to determine whether similar mitochondrial changes occur in peripheral cells using fibroblasts from nine lines of sAD patients and nine lines of age-matched normal controls. NHFs and sAD fibroblasts, which had similar growth rates at similar cumulative population doubling levels (CPDL 16 to 18) were plated to 60% to 80% confluence on chamber slides coated with fibronectin one day before transfection. Twenty-four

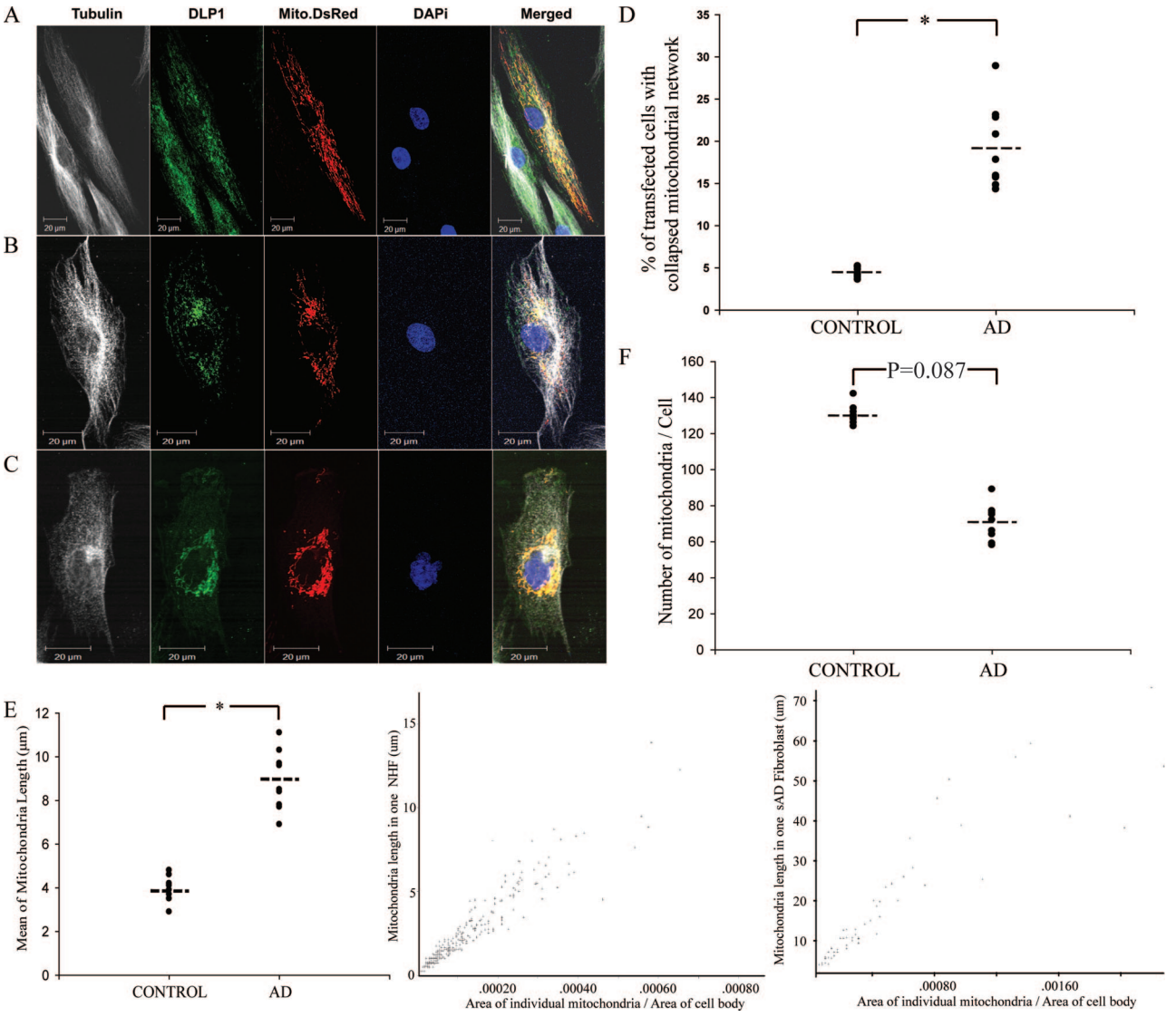

Figure 1. sAD fibroblasts demonstrate abnormal mitochondrial distribution and morphology compared to NHFs. **A–C:** Three distinct patterns of mitochondrial distribution were seen in fibroblasts. Representative fluorescence images show mitochondria (red), DLP1 (green), α-tubulin (white) and nuclear (blue). In the majority of NHFs (>95%), mitochondria are evenly distributed throughout the cytoplasm (**A**). In approximately 20% of sAD fibroblasts, the mitochondrial network is partially collapsed with the majority of mitochondria clustering around the perinuclear area (**B**). In approximately 2% of sAD fibroblasts, the mitochondrial network is completely collapsed with all mitochondria densely clustering around the nucleus (**C**). **D:** Quantitative analysis revealed significantly more sAD fibroblasts displaying an abnormal mitochondrial distribution pattern (**B** and **C**) compared to NHFs ($P < 0.05$). **E:** sAD fibroblasts with normal mitochondrial distribution pattern also demonstrate significantly elongated mitochondria compared to NHFs (left panel) ($P < 0.05$). Center and right panels show the typical distribution of mitochondrial length versus mitochondrial size for a typical NHF (center panel) and sAD fibroblast with a normal mitochondrial distribution pattern (right panel). **F:** There is a trend of decreased mitochondrial number in sAD fibroblasts with normal mitochondrial distribution pattern compared to that of NHFs ($P = 0.087$).

hours after being transfected with mito-DsRed2, cells were fixed, stained, visualized by laser confocal microscope, and mitochondrial parameters analyzed in Mito-DsRed2 positively transfected cells. Mitochondria were evenly distributed throughout the cytoplasm (Figure 1A) in the majority of NHFs (>95%). However, in marked contrast, significant numbers of sAD fibroblasts (19.34 ± 1.64%, $P < 0.001$) in each of the sAD lines demonstrated an abnormal distribution of mitochondria with a partially collapsed mitochondrial network (Figure 1, B and D), ie, at least 60% mitochondria clustered around the perinuclear area, defined as having a radius twofold the length of the longer arm of the nucleus (see Supplemental Figure S1 at *http://ajp.amjpathol.org*). In fact, some sAD fibroblasts (2.07 ± 0.25%) even exhibited a completely collapsed mitochondria network, ie, at least 95% of the mitochondria clustering around the perinuclear area with a complete loss of mitochondria at more remote regions of the cell (Figure 1C).

To determine whether the observed mitochondrial distribution abnormality was due to an altered ratio of cells at different cell cycle phases, the cell cycle distribution pattern in NHFs and sAD fibroblasts was measured by flow cytometric analysis, and no significant difference was found (not shown), consistent with a previous report.[31] In addition, NHFs and sAD fibroblasts were synchronized by serum starvation or hydroxyurea treatment. Cell cycle synchronization was confirmed by propridium

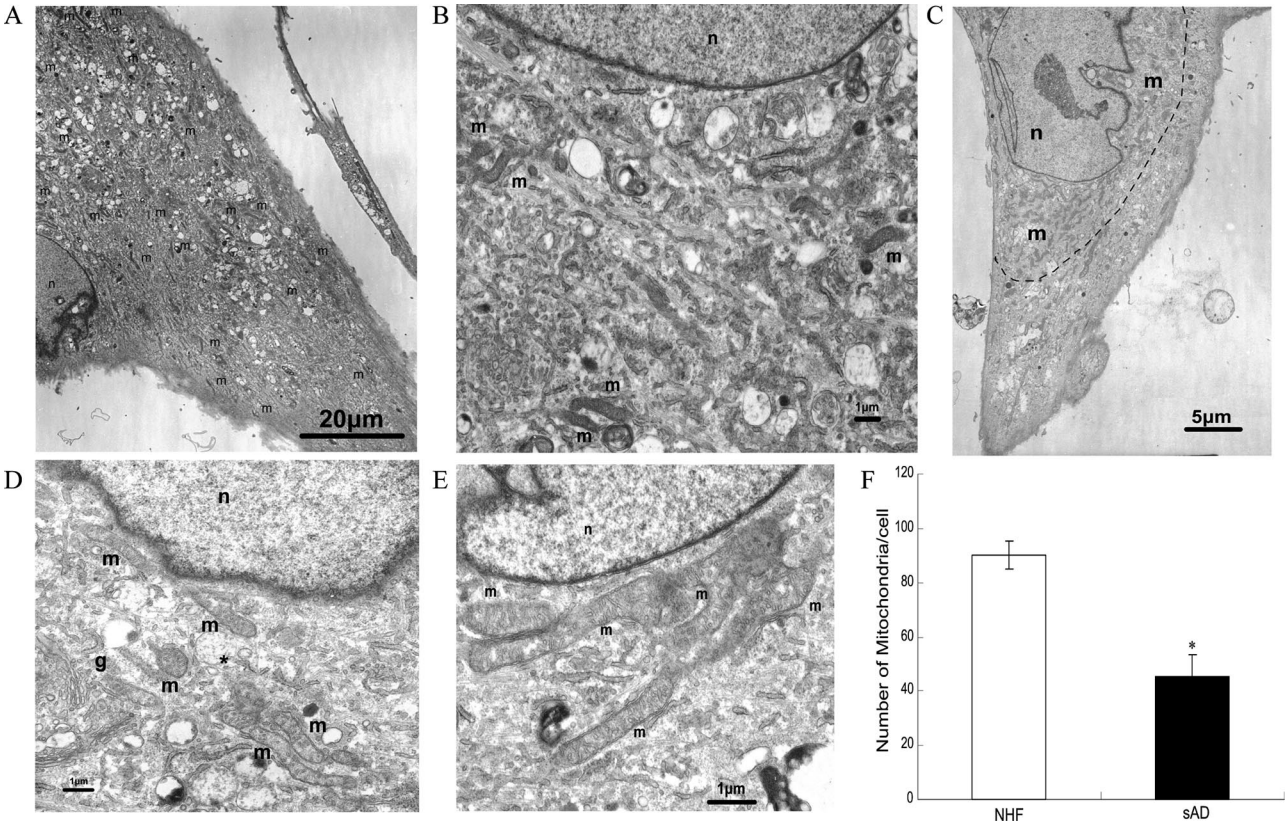

Figure 2. EM analysis of abnormal mitochondrial distribution and morphology in sAD fibroblasts compared to NHFs. **A** and **B:** Representative micrographs of NHFs. **A:** Evenly distributed mitochondria (m) in NHF. **B:** Higher magnification showing normal distribution and morphology of mitochondria in NHF. **C–E:** Representative micrographs of sAD fibroblasts. **C:** Mitochondria (m) clustered around the nucleus (n). Elongated and branched mitochondria in the perinuclear area are clearly visible at higher magnification (**D** and **E**). Golgi apparatus (g) is present in **D**. The small round mitochondrion (*) found in **D** might result from a transverse section of a cylindrical mitochondrion. **F:** Quantitative analysis revealed significantly fewer mitochondria in sAD fibroblasts compared to NHFs (*$P <$ 0.05; Student's *t*-test). Moreover, those in the former cells exhibited a restricted distribution.

iodide/RNase staining 24 hours or 72 hours after addition of serum or removal of hydroxyurea. The mitochondria distribution pattern remained the same in synchronized cells such that the abnormal ratio in NHFs was 3.93 ± 1.1% in contrast to 20.45 ± 2.35% in sAD fibroblasts (not shown).

We also measured mitochondrial length in mito-DsRed2-transfected cells. Quantification of 100 randomly selected cells per line that showed a normal mitochondria distribution pattern revealed that the mean mitochondrial length of 9.3 ± 2.3 μm (mean ± SEM) in sAD fibroblasts was significantly greater than the mean length of 4.5 ± 2.1 μm in NHFs ($P < 0.01$) (Figure 1E, left panel). Figure 1E, center and right panels, shows the individual mitochondrial morphology parameters in representative NHF or sAD fibroblasts. Mitochondrial length and size are significantly increased in sAD fibroblasts compared to NHF. Noteworthy is that the extremely long mitochondria (>30 μm) shown in sAD fibroblast (Figure 1E, right panel) appear to reflect highly connected networks of two or more branched or tubular mitochondria. While there was a trend toward a decrease in mitochondria number in sAD fibroblasts with normal mitochondrial distribution, this did not reach significance ($P = 0.087$) (Figure 1F).

In those sAD fibroblasts with a collapsed mitochondrial network (Figure 1, B and C), it was very difficult to measure their mitochondrial length and number using confocal microscopy techniques because the mitochondria were clustered. Therefore we investigated these cells (three lines of NHFs and three lines of sAD fibroblasts) using electron microscopy and, consistent with our findings by confocal microscopy, NHFs show mitochondria evenly dispersed throughout the cytoplasm with an average length of 2.6 ± 0.71 μm, which appeared sausage- or round-shaped (depending on the angle of cutting through the mitochondria body) (Figure 2, A and B). In contrast, in many sAD fibroblasts, mitochondria clustered around the perinuclear area (Figure 2C) and morphologically were much longer (6.5 ± 1.4 μm, $P < 0.01$), often forming branch-like structures (Figure 2, D and E). Importantly, the number of mitochondria was significantly decreased in sAD fibroblasts with a collapsed mitochondrial network as compared to NHFs (Figure 2F, $P < 0.01$).

DLP1 Level Change in sAD Fibroblasts

Because mitochondrial fission and fusion proteins regulate mitochondrial morphology and distribution,[17] we investigated whether DLP1, a mitochondrial fission protein, and OPA1, a mitochondrial fusion protein, was involved in the abnormal changes of mitochondrial distribution and

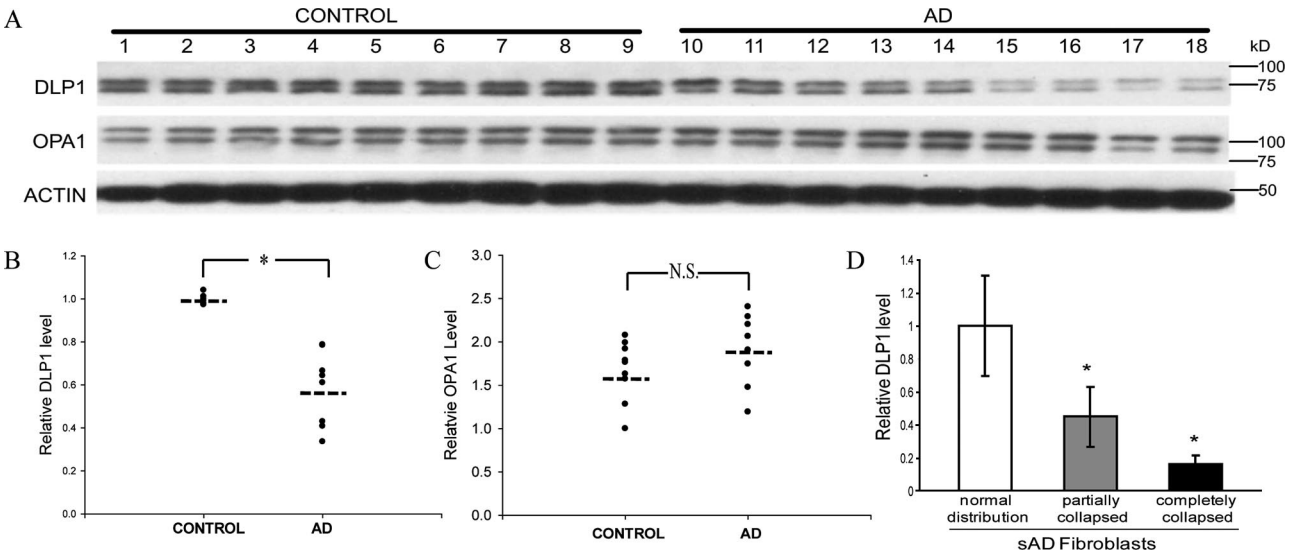

Figure 3. The level of DLP1 changes in sAD fibroblasts. **A:** A representative immunoblot of cell lysates of sAD fibroblasts and age-matched NHFs probed with antibody against DLP1. A parallel blot was probed with antibody against OPA1. The same membranes were stripped and reprobed with actin antibody as an internal loading control. Equal protein amounts (20 μg) were loaded. **B** and **C:** Quantification of the DLP1 or OPA1 reactive bands, normalized to actin levels, reveals significantly decreased levels of DLP1 but no changes in OPA1 levels in sAD fibroblasts ($n = 9$) compared to age-matched NHFs ($n = 9$). **D:** sAD fibroblasts with abnormal mitochondrial distribution demonstrate greater reduction in DLP1 levels compared to those with a normal mitochondrial distribution pattern. DLP1 levels in individual sAD fibroblasts were measured based on quantification of DLP1 fluorescent immunoreactivity (*$P < 0.05$; N.S., not significant, Student's *t*-test).

morphology observed in sAD fibroblasts. By immunoblot analysis, DLP1 levels were significantly ($P < 0.05$) reduced by 42% in sAD fibroblasts compared to NHFs (Figure 3, A–C), but no significant changes in OPA1 levels were observed. More interestingly, quantification of DLP1 fluorescent immunoreactivity in sAD fibroblasts revealed a large variation in DLP1 levels in sAD fibroblasts; those cells with abnormal mitochondrial distribution demonstrated significantly greater reduction in DLP1 levels compared to those with normal mitochondrial distribution in the same sAD fibroblast line (Figure 3D). These correlative analyses suggest that a reduction in DLP1 may be involved in the abnormal mitochondrial morphology and distribution in sAD fibroblasts.

Dominant Negative Mutant DLP1 or DLP1 Knockdown Results in Mitochondrial Network Collapse in NHF

To test the hypothesis that DLP1 reduction causes abnormalities in mitochondrial distribution and morphology, we determined the effect of DLP1 knockdown in NHFs. We transfected six lines of NHFs (CPDL: 16 ~ 20) with green fluorescent protein-tagged miR RNAi expression vector targeted to DLP1, and cells were examined 48 hours after transfection. Positively transfected cells identified by GFP staining demonstrated an approximately 40% transfection efficiency. Consistent with this, immunoblot analysis revealed a 30% decrease in DLP1 levels in transfected cultures (Figure 4, A and B). In positively transfected cells, the ratio of cells with mitochondria clustering around the perinuclear area was significantly increased to around 31.0 ± 5.2% compared to no more than 5% of nontransfected cells or empty-vector-transfected cells (Figure 4C) (representative pictures of positively transfected NHFs with normal/abnormal mitochondrial distribution are shown in Supplemental Figure S2 at *http://ajp.amjpathol.org*). We also transfected three lines of NHFs (CPDL: 16 ~ 20) with hemagglutinin (HA)-tagged DLP1-K38A, a dominant negative mutant. Forty-eight hours after transfection, cells were fixed and stained with mouse anti-HA antibody to identify the positively transfected cells. In positively transfected cells, the ratio of cells with mitochondria clustering around the perinuclear area was significantly increased to 19.5 ± 4.6%, compared to vehicle-transfected NHFs and was more comparable to sAD fibroblasts (Figure 4C). Furthermore, by analyzing mitochondrial length in positively transfected fibroblasts with normal mitochondrial distribution by confocal microscopy, we found that overexpression of the dominant negative mutant DLP1-K38A or knockdown of DLP1 led to a significant elongation of mitochondria (Figure 4D), similar to that found in sAD fibroblasts. Finally, mitochondria number in transfected cells was also significantly decreased (Figure 4E).

Mitochondrial Network Collapse in sAD Fibroblasts Could Be Rescued by Overexpression of Wild-Type DLP1

To determine whether mitochondrial abnormalities in sAD fibroblasts could be rescued by overexpressing wild-type DLP1, we transfected five lines of sAD fibroblasts (PD: 16 ~ 20) with HA-tagged wild-type DLP1. Consistent with a previous study,[17] the viability of cells was not affected by overexpression of wild-type DLP1. Forty-eight hours after transfection, cells were fixed and immunostained with mouse anti-HA antibody to identify DLP1 positively transfected cells (representative pictures of positively transfected sAD fibroblasts with normal or ab-

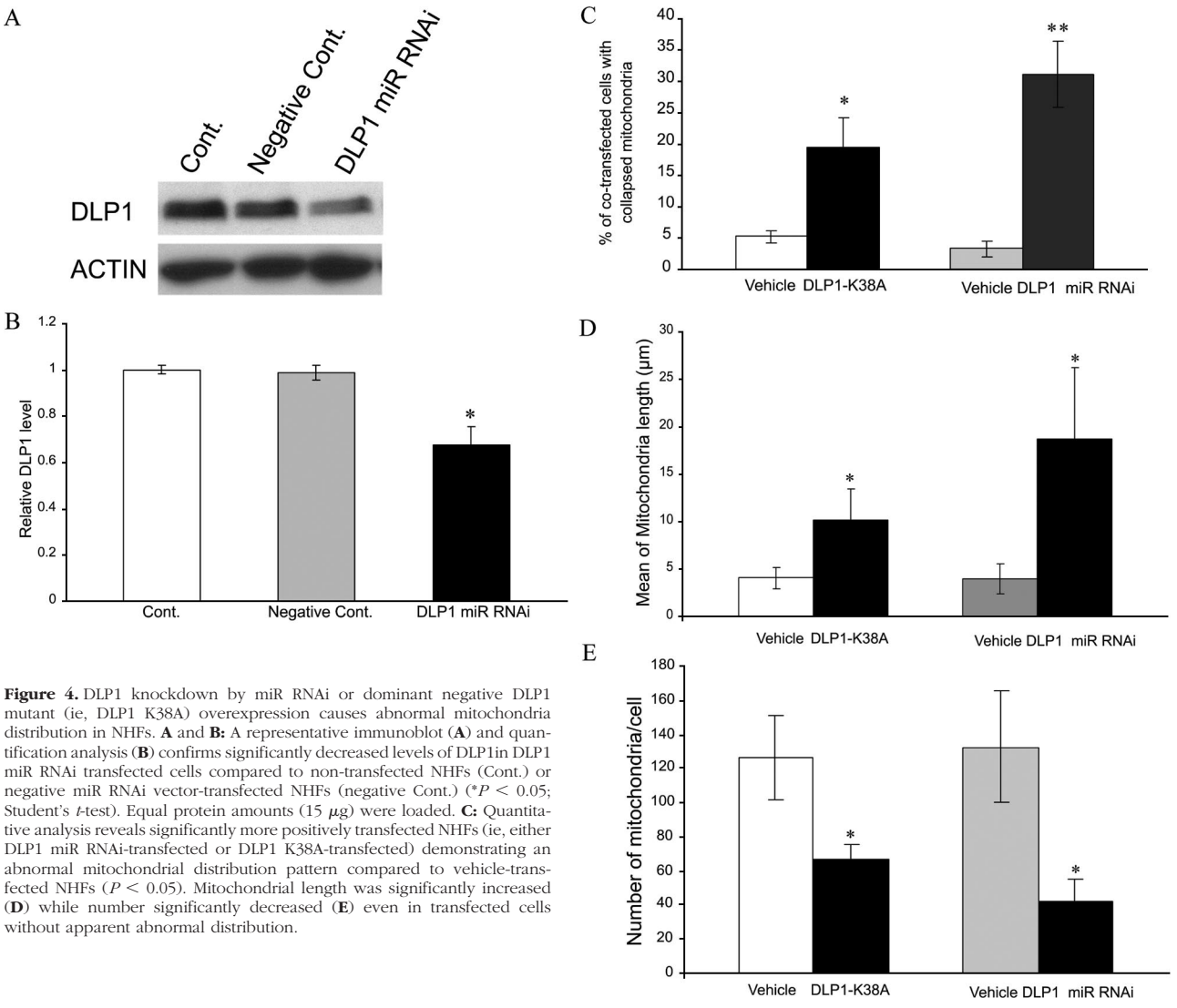

Figure 4. DLP1 knockdown by miR RNAi or dominant negative DLP1 mutant (ie, DLP1 K38A) overexpression causes abnormal mitochondria distribution in NHFs. **A** and **B:** A representative immunoblot (**A**) and quantification analysis (**B**) confirms significantly decreased levels of DLP1in DLP1 miR RNAi transfected cells compared to non-transfected NHFs (Cont.) or negative miR RNAi vector-transfected NHFs (negative Cont.) (*$P < 0.05$; Student's *t*-test). Equal protein amounts (15 μg) were loaded. **C:** Quantitative analysis reveals significantly more positively transfected NHFs (ie, either DLP1 miR RNAi-transfected or DLP1 K38A-transfected) demonstrating an abnormal mitochondrial distribution pattern compared to vehicle-transfected NHFs ($P < 0.05$). Mitochondrial length was significantly increased (**D**) while number significantly decreased (**E**) even in transfected cells without apparent abnormal distribution.

normal mitochondrial distribution are shown in Supplemental Figure S3 at *http://ajp.amjpathol.org*). Consistent with a role for DLP1 in mitochondrial distribution, the ratio of cells with mitochondria clustering around the perinuclear area significantly decreased from 16.5% ± 1.5% in vehicle-transfected or control cells to 8.9% ± 1.3% in DLP1-transfected cells (Figure 5A). Moreover, the mean mitochondrial length in sAD fibroblasts (9.0 ± 1.8 μm) was significantly decreased by overexpression of HA-tagged DLP1 (3.0 ± 1.2 μm), comparable to that of NHFs (4.5 ± 2.1 μm) (Figure 5B). Mitochondria number in HA-tagged DLP1 overexpressing sAD fibroblasts also

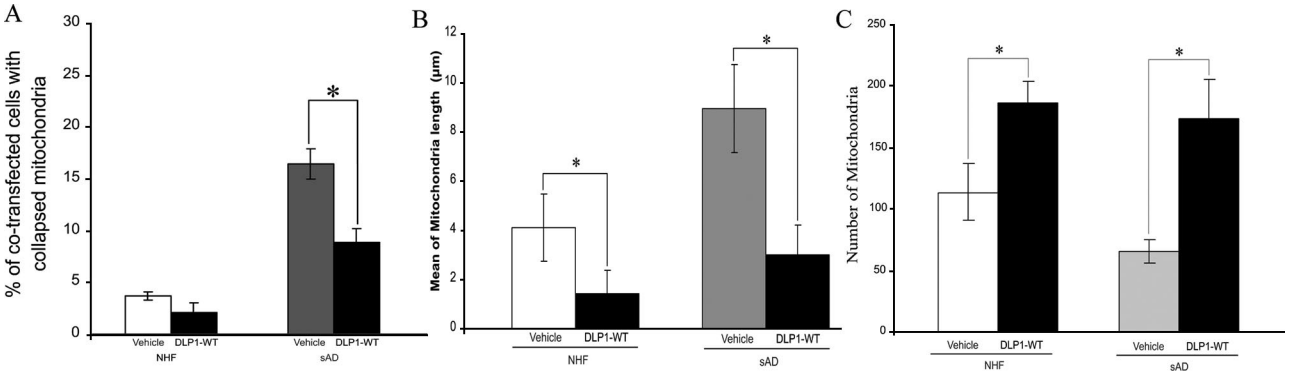

Figure 5. Overexpression of wild-type DLP1 rescues abnormal mitochondria distribution (**A**) and morphology (**B**) and increased mitochondrial number (**C**) in sAD fibroblasts.

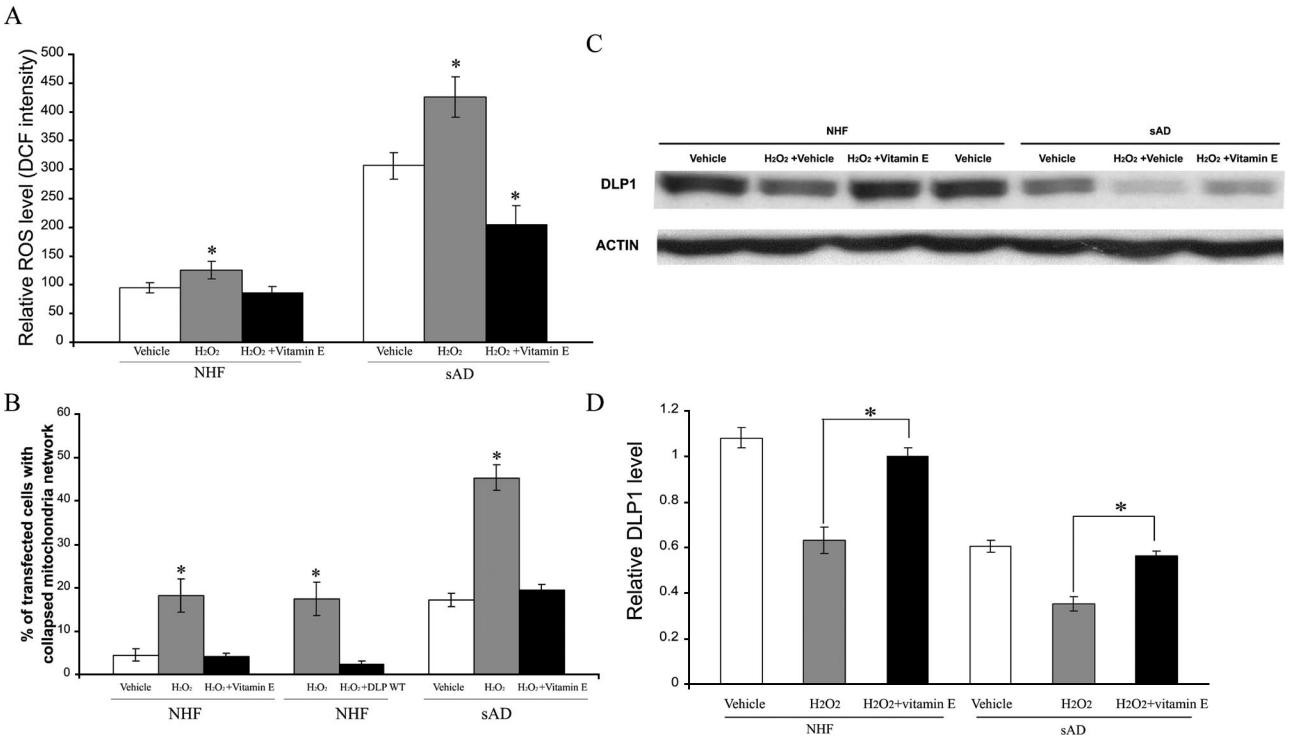

Figure 6. Hydrogen peroxide causes mitochondrial abnormalities and changes levels of DLP1 in NHFs and exacerbated that of sAD fibroblasts, and can be abolished by vitamin E pretreatment. **A:** ROS levels in NHFs and sAD fibroblasts (*$P < 0.05$ compared to vehicle without H_2O_2 treatment. **B:** Significantly more NHFs and sAD fibroblasts demonstrate an abnormal mitochondrial distribution pattern with mitochondrial clustering around the nucleus after hydrogen peroxide treatment, which was totally abolished by vitamin E pretreatment. WT DLP1 overexpression prevents hydrogen peroxide-induced mitochondrial network collapse. A representative immunoblot (**C**) and quantification analysis (**D**) demonstrates that hydrogen peroxide-induced DLP1 reduction in NHFs and further reduction in sAD fibroblasts is abrogated by vitamin E pretreatment.

significantly increased (Figure 5C). Notably, DLP1 overexpression in NHFs also led to decreases in the ratio of cells with abnormal mitochondrial distribution, mitochondrial length, and increased mitochondrial numbers (Figure 5, A–C). These findings further confirm that the abnormal mitochondrial morphology and distribution observed in sAD fibroblasts can be rescued by overexpression of DLP1.

Oxidative Stress Causes Abnormal Mitochondrial Distribution in NHFs and Exacerbates That in sAD Fibroblasts

Oxidative stress is one of the prominent pathogenic factors of AD that affects both neuronal and peripheral cells.[28,35] Consistent with previous studies,[36] we found that cellular ROS levels are increased threefold in sAD fibroblasts compared to NHFs (Figure 6A, $P < 0.05$). To determine whether ROS are involved in DLP1 reduction and mitochondrial abnormalities, we plated sAD fibroblasts (three lines, CPDL: 16 ~ 20) or age-matched NHF (three lines, CPDL: 16 ~ 20) on chamber slides coated with fibronectin and then transfected with mito-DsRed2. Twenty-four hours after transfection, cells were treated with 50 μmol/L H_2O_2 for 1 hour and examined after 3 hours of recovery. No obvious cell death was observed in either NHFs or sAD fibroblasts under these conditions as determined by lactate dehydrogenase assay (data not shown). Nonetheless, H_2O_2 treatment caused significantly increased intracellular ROS levels (Figure 6A) and increased the ratio of cells with a collapsed mitochondrial network in NHFs (ie, from 4.4 ± 1.4% in untreated cells to 18.1 ± 3.8% in treated cells, $P < 0.05$%) (Figure 6B) (representative pictures of H_2O_2-treated NHFs with normal and abnormal mitochondrial distribution are shown in Supplemental Figure S4 at *http://ajp.amjpathol.org*). Interestingly, H_2O_2 treatment leads to even greater increases in the ratio of cells with a collapsed mitochondrial network in sAD fibroblasts (ie, from 17.1 ± 1.6% in untreated cells to 45.3 ± 2.8% in treated cells, $P < 0.05$%) (Figure 6B). Since H_2O_2 can induce cellular senescence, to determine whether senescence plays any role in our observations, senescence-associated β-galactosidase assay was performed and the β-galactosidase-positive cells were counted and the percentage was calculated. There was no difference in the percentage of senescent cells between NHFs and sAD fibroblasts nor between H_2O_2-treated and -untreated cells (not shown), suggesting that senescence is not a factor contributing to our observations. Consistent with a key role of DLP1 in mitochondrial network collapse, H_2O_2 treatment resulted in a significant decrease in DLP1 levels in NHFs and an additional decrease in sAD fibroblasts (Figure 6, C and D). In fact, there was a significant negative correlation between levels of intracellular ROS and DLP1 ($r = 0.87$, $P < 0.05$) and between DLP1 levels and the ratio of cells with an abnormal mitochondrial distribution ($r = 0.88$, $P < 0.05$). Notably, decreases in DLP1 occurred as early as 30

minutes after H_2O_2 treatment when no apparent mitochondrial network collapse was observed in either NHFs or sAD fibroblasts (data not shown). To further determine causality, NHFs transiently transfected with WT DLP1 were treated with H_2O_2 and the ratio of cells with abnormal mitochondrial distribution in those WT DLP1 positively transfected NHFs is 2.2 ± 0.9% compared to 17.4 ± 3.9% in those nontransfected cells in the same culture (Figure 6B). This strongly supports the involvement of DLP1 reduction in mediating the abnormal mitochondrial distribution induced by H_2O_2. In addition, pretreatment of cells with vitamin E, which effectively prevents H_2O_2-induced intracellular ROS increase (Figure 6A), completely inhibited the H_2O_2-induced abnormal mitochondria distribution and DLP1 decrease in both NHFs and sAD fibroblasts (Figure 6, B–D).

Overexpression of Wild-Type APP or Swedish Mutant APP in NHFs Causes Abnormal Mitochondrial Distribution

Mutations in APP cause AD presumably through alterations in amyloid β (Aβ) production and, since both APP and Aβ are present in the mitochondria, may exert deleterious effect on mitochondrial function.[37–40] We therefore determined the effect of overexpression of WT or familial AD-causing APPswe on mitochondrial distribution and DLP1. In NHFs overexpressing WT APP, the ratio of cells with a collapsed mitochondrial network was increased significantly (ie, 20.6 ± 6.4%) compared to vehicle-transfected cells and nontransfected cells (Figure 7A) (representative pictures of APP positively transfected NHFs with normal/abnormal mitochondrial distribution are shown in Supplemental Figure S5 at *http://ajp.amjpathol.org*). Importantly, this ratio was further greatly increased to 43.1 ± 7.9% in NHFs overexpressing APPswe (Figure 7A). The overexpression of WT APP or APPswe in NHFs also resulted in a significant decrease in DLP1 protein levels, paralleling abnormal changes in mitochondrial distribution (Figure 7B). To determine whether APP-induced DLP1 reduction underlies the APP-induced abnormal mitochondrial distribution, a cotransfection experiment was performed. The overexpression of WT DLP1 completely prevents the APP overexpression-induced abnormal mitochondrial distribution (Figure 7A). These data strongly support the involvement of DLP1 reduction in mediating abnormal mitochondrial distribution induced by APP overexpression.

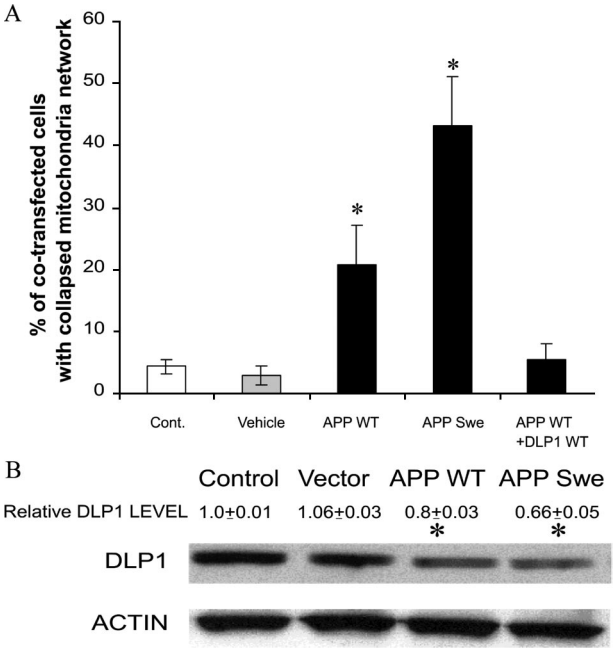

Figure 7. Overexpression of wild-type APP or APP Swedish mutant (APPswe) causes abnormal mitochondrial distribution in NHFs (**A**) and reduction of DLP1 levels (**B**). Concurrent overexpression of WT DLP1 prevents APP overexpression-induced mitochondrial network collapse (**A**), $P < 0.05$.

Discussion

In this study, we show a significant increase in abnormal mitochondrial morphology and distribution in fibroblasts from sAD compared to age-matched NHFs. Specifically, mitochondria were significantly longer and clustered around the perinuclear area in many sAD fibroblasts. The difference in mitochondrial distribution is not likely due to different phases during cell cycle, since there was no significant difference in the distribution pattern of cells at different cell cycle phases between sAD fibroblasts and NHFs, nor were there differences after cell cycle synchronization. However, by manipulating the expression of DLP1, the mitochondrial fission protein that regulates mitochondrial morphology and distribution, we demonstrated that the mechanism underlying mitochondrial abnormalities in sAD fibroblasts appears to involve ROS-dependent and/or Aβ-dependent reduction in DLP1.

DLP1 Reduction Underlies Mitochondrial Changes in sAD Fibroblasts

The major observation of this study is that mitochondria demonstrate abnormal changes in morphology and distribution in a significant number of sAD fibroblasts. It remains to be determined whether these abnormalities contribute to peripheral, non-neuronal manifestations in AD. Two factors likely complicate our discussion: 1) the abnormal mitochondrial morphology and distribution are observed in approximately 20% sAD fibroblasts; and 2) we have measured mitochondrial membrane potential as a mitochondrial functional parameter but failed to find significant difference between sAD and control fibroblasts (not shown), which is consistent with previous studies. Furthermore, we also failed to find any significant difference in mitochondrial membrane potential between sAD fibroblasts with abnormal mitochondria and sAD fibroblasts with normal mitochondria (not shown), which is not unexpected since manipulations of mitochondrial fission/fusion proteins in fibroblasts that cause changes in mitochondrial morphology and distribution do not necessarily cause changes in mitochondrial membrane potential.[41] Even though a more subtle functional conse-

quence such as deficiency of local ATP production cannot be ruled out, it is not clear whether such subtle functional consequences in approximately 20% of fibroblasts will make a peripheral manifestation in AD patients. Nevertheless, our findings demonstrated for the first time that mitochondrial fission and fusion imbalance occurs in cells from AD patients and, given the potential adverse effects of these mitochondrial abnormalities in polarized cells like neurons, suggested more detailed scrutiny of this aspect of mitochondrial parameters in affected neurons are needed.

Mitochondria were significantly longer in sAD fibroblasts as evidenced by both confocal and electron microscopy. There were also extremely long mitochondria in sAD fibroblasts, reflecting highly connected networks of two or more branched mitochondria. These findings suggested that the balance of mitochondria fission and fusion, a process that controls mitochondria morphology, is tipped toward less fission. Indeed, we found reduced levels of DLP1, a mitochondrial fission protein, but no changes in the levels of OPA1, a mitochondrial fusion protein, in sAD fibroblasts. Moreover, in contrast to the even distribution throughout the cytoplasm in the majority of NHFs, mitochondria were clustered around the perinuclear area in around 20% of the sAD fibroblasts and, in fact, mitochondria number was also significantly decreased in these cells. Among the proteins involved in mitochondrial fission/fusion, DLP1 is also involved in the regulation of mitochondria distribution.[17] In this regard, we found significantly decreased levels of DLP1 in sAD fibroblasts, especially in those cells with abnormal mitochondrial distribution, consistent with reduced fission in these cells, suggesting a potential involvement of DLP1 reduction in mitochondrial changes in sAD fibroblasts. Further, we found a significant negative correlation between DLP1 levels and cells with abnormal mitochondrial distribution changes. The fact that DLP1 knockdown and expression of dominant negative DLP1 in NHFs caused changes in mitochondrial morphology and distribution comparable to those seen in sAD fibroblasts and the fact that overexpression of wild-type DLP1 rescues the abnormal mitochondrial morphology and distribution in sAD fibroblasts strongly suggests that DLP1 reduction causes mitochondrial abnormalities in sAD fibroblasts. Notably, fibroblasts from Parkinson's disease patients bearing PINK-1 mutations also demonstrated abnormal mitochondrial morphology,[42] which is likely due to decreased DLP1 function,[43] suggesting that abnormal mitochondrial dynamics may be a common pathway leading to cellular dysfunction critical to different neurodegenerative diseases.

That only approximately 20% of sAD fibroblasts demonstrated abnormal changes in mitochondrial distribution likely reflects the fact that human fibroblasts are heterogeneous cell populations. Indeed, despite the significant overall reduction in DLP1 levels in sAD fibroblasts compared to NHFs as shown by immunoblot, levels of DLP1 in different cells in the same line of heterogeneous population of sAD fibroblasts are likely different as evidenced by the large variation in DLP1 levels based on the quantification of DLP1 fluorescent immunoreactivity in sAD fibroblasts. In fact, DLP1 levels in those sAD fibroblasts with a partially collapsed mitochondrial network were only approximately 50%, while in those sAD fibroblasts with a completely collapsed mitochondrial network were approximately 20% of the DLP1 levels in those cells with normal distribution. Therefore, we suspect that only those sAD fibroblasts with the most severe reduction in DLP1 levels, on reaching a certain threshold, demonstrate the phenotype of abnormal mitochondrial distribution, which accounts for the observation that only a subset of the fibroblasts from AD demonstrate abnormalities. In support of this notion, several stable lines of M17 cells with different residual expression levels of DLP1 after miR RNAi knockdown were established and mitochondrial network analyzed. We found that significant mitochondrial distribution abnormalities begin to occur only when DLP1 levels drop below 65%, and the severity negatively correlates with residual DLP1 levels such that those cells with nearly 20% residual DLP1 demonstrate a complete collapsed mitochondrial network (X. Wang and X. Zhu, unpublished results).

ROS and APP Overexpression Cause DLP1 Reduction and Abnormal Mitochondrial Distribution

As a potential pathogenic factor, oxidative stress is one of the earliest prominent features in AD and affects both neuronal cells and peripheral cells.[28,35] Indeed, sAD fibroblasts demonstrated 3 times higher basal level cellular ROS than NHFs, even though they were maintained at a similar condition *in vitro*. A likely source for increased oxidative stress in sAD fibroblasts is abnormal mtDNA in AD peripheral cells, since sAD cybrids demonstrated heightened ROS levels compared to control cybrids.[44] It is known that mitochondrial dynamics can be affected by ROS. In this study, we found that 50 μmol/L H_2O_2 treatment, which increases cellular ROS in NHFs, induced DLP1 reduction and altered mitochondrial distribution comparable to sAD fibroblasts. H_2O_2 treatment induced a further increase in ROS levels in sAD fibroblasts accompanied by a further decrease in DLP1 levels and even greater mitochondrial abnormalities. Indeed, there is a significant negative correlation between ROS levels and DLP1 levels and also a significant negative correlation between DLP1 levels and cells with mitochondrial changes. Moreover, DLP1 reduction occurs before changes in mitochondrial distribution. Most importantly, DLP1 overexpression completely prevented H_2O_2-induced abnormal mitochondrial distribution. Moreover, vitamin E pretreatment rescued the DLP1 reduction and the mitochondrial changes induced by H_2O_2 in treated NHFs and sAD fibroblasts. Based on these data, we conclude that external oxidative stress causes DLP1 reduction that in turn causes abnormal mitochondrial distribution. While apoptosis can affect mitochondrial fission/fusion,[45] DLP1 reduction and mitochondrial changes observed in both NHFs and sAD fibroblasts induced by H_2O_2 are unlikely due to apoptotic effect, since this level of H_2O_2 was insufficient to induce cell death in either

NHFs or sAD fibroblasts. The lack of cell death is further evidenced by the fact that abnormal mitochondrial distribution can be reversed in these cells after 24 hours when H_2O_2 was cleared by cells from medium (not shown). Since there was no difference in the percentage of senescent cells in our experiments, H_2O_2-induced cellular senescence is unlikely a contributing factor to abnormal mitochondrial distribution. The characterization of mechanisms of how ROS induces DLP1 reduction is currently underway in our laboratory.

Finally, we found that overexpression of WT APP and familial AD-causing APP mutant also induces DLP1 reduction and mitochondrial network collapse. The characterization of mechanisms underlying APP-induced DLP1 reduction obviously warrants further investigation. Since APP is present in mitochondria,[37,38] APP overexpression may directly interfere with mitochondrial fission and fusion balance. Recent evidence suggested that mutant APP may block mitochondrial import channels and affect mitochondrial function[38] that may indirectly affect mitochondrial dynamics. Another possible mechanism is through the increased Aβ production. Indeed, we found that Aβ_{1-42} caused reduced DLP1 levels in M17 cells in a dose- and time-dependent manner (X. Wang and X. Zhu, unpublished results). Aβ may exert its adverse effect on mitochondria through multiple mechanisms. First, since Aβ is present in mitochondria,[39,40] it is possible that Aβ directly induces mitochondrial changes. Also, since Aβ is a well defined intrinsic ROS generator, it is possible that Aβ induces DLP1 reduction and mitochondrial changes via ROS production. Nevertheless, the possible involvement of other mechanisms cannot be excluded. In this regard, it is worth mentioning that Aβ causes cleavage of dynamin, a protein related to DLP1, by inducing calpain activation.[46] Moreover, Aβ may also indirectly affect DLP1 and mitochondria; for example, excessive Aβ binds to regulatory heme that triggers functional heme deficiency and indirectly causes mitochondrial dysfunction.[30,47,48] Nevertheless, involvement of other cleavage products of APP in APP-induced DLP1 reduction and mitochondrial network collapse also cannot be ruled out at this time. These mechanisms may also play a role in sporadic AD cases, since sAD cybrids secrete twice as much Aβ_{1-40} and Aβ_{1-42}, have increased intracellular Aβ_{1-40} (1.7-fold), and develop Congo red-positive Aβ deposits,[44] suggesting that it is possible APP metabolism may be different in sAD peripheral cells and thus contribute to DLP1 reduction and mitochondrial abnormalities in these cells.

DLP1 Reduction, Mitochondria Changes, and Their Functional Significance and Implications in Neurodegeneration

Mitochondrial function largely relies on a highly dynamic balance of both morphology and distribution, which can be affected by cellular redox status.[49] In this regard, sAD fibroblasts demonstrated 3 times higher basal level cellular ROS than NHFs, which suggests that sAD fibroblasts are exposed to a chronic and low dose of oxidative stress. Notably, these cells are more resistant to ROS-induced apoptosis,[50] suggesting that they achieve an altered redox homeostasis with a heightened basal intracellular level of ROS presumably by provoking some adaptive responses. Interestingly, up-regulation of DLP1 and excessive mitochondria fission is implicated in apoptosis,[51] while down-regulation of DLP1 renders cells more resistant to apoptosis.[52,53] Thus, it is possible that sAD fibroblasts, by down-regulating DLP1 and decreasing mitochondrial fission in response to chronic oxidative stress, effectively lower their susceptibility to further increases in oxidative stress. In addition, mitochondrial elongation and increased fusion in sAD fibroblasts could decrease mitochondria respiration rate and diminish ROS production,[54] which would effectively lower the oxidative stress in such a chronic situation. Therefore, DLP1 reduction and mitochondrial elongation in sAD fibroblasts may serve as a protective adaptation to chronic oxidative stress. In this regard, it is thought that susceptible neurons in AD are also subject to chronic oxidative stress.[55] Likely not coincidentally, mitochondria are also significantly decreased and larger in these neurons,[9] and our preliminary results show that DLP1 is also decreased in AD brains compared to age-matched controls (not shown), suggesting a similar adaptive mechanism in response to chronic oxidative stress in these susceptible neurons. However, it must be emphasized that reductions in DLP1 levels, presumably once reaching a certain threshold, also results in changes in mitochondrial distribution. Although no significant differences in mitochondrial membrane potential were found in those sAD fibroblasts with abnormal mitochondrial distribution compared to those with normal mitochondrial distribution (not shown), a more subtle functional consequence such as deficiency of local ATP production cannot be ruled out. This may not be a problem for fibroblasts, however, given that neurons are extremely polarized cells that rely heavily on mitochondria for energy support for local needs,[18] it is possible that DLP1 reduction, despite its beneficial effect on reducing ROS and apoptosis, would have deleterious effect on mitochondrial distribution in remote neuronal structures such as synapses. In this regard, others found that expression of DLP1 dominant negative mutant that causes depletion of mitochondria from remote sites such as synapse leads to subtle changes in Ca^{2+} buffering in synapses following nerve stimulation maintained at high intensity for extended time periods that appears to be due to a dysfunctional subpopulation of synaptic vesicles, the reserve pool, and can be partially rescued by exogenous ATP in DLP1 mutant *Drosophila*.[56] Reduced expression of DLP1 or expression of DLP1 dominant negative mutant also causes depletion of mitochondria from dendrites, which leads to loss of synapses and dendritic spines.[18] Indeed, among all of the early changes that occur in AD, synaptic loss is the more robust correlate of AD-associated cognitive deficits,[57] leading to the notion that synaptic dysfunction plays a critical role in the pathogenesis of AD.[58] Therefore, the functional significance of mitochondrial distribution as well as fission/fusion balance in AD neurons and its potential contribution to synaptic dysfunction and neuronal degeneration warrants further investigation.

References

1. Smith MA: Alzheimer disease. Int Rev Neurobiol 1998, 42:1–54
2. Nunomura A, Perry G, Aliev G, Hirai K, Takeda A, Balraj EK, Jones PK, Ghanbari H, Wataya T, Shimohama S, Chiba S, Atwood CS, Petersen RB, Smith MA: Oxidative damage is the earliest event in Alzheimer disease. J Neuropathol Exp Neurol 2001, 60:759–767
3. Liu J, Ames BN: Reducing mitochondrial decay with mitochondrial nutrients to delay and treat cognitive dysfunction, Alzheimer's disease, and Parkinson's disease. Nutr Neurosci 2005, 8:67–89
4. Liu J, Head E, Gharib AM, Yuan W, Ingersoll RT, Hagen TM, Cotman CW, Ames BN: Memory loss in old rats is associated with brain mitochondrial decay and RNA/DNA oxidation: partial reversal by feeding acetyl-L-carnitine and/or R-alpha-lipoic acid, Proc Natl Acad Sci USA 2002, 99:2356–2361
5. Blass JP, Sheu RK, Gibson GE: Inherent abnormalities in energy metabolism in Alzheimer disease. Interaction with cerebrovascular compromise. Ann NY Acad Sci 2000, 903:204–221
6. Swerdlow RH, Kish SJ: Mitochondria in Alzheimer's disease. Int Rev Neurobiol 2002, 53:341–385
7. Zhu X, Wang Y, Ogawa O, Lee HG, Raina AK, Siedlak SL, Harris PL, Fujioka H, Shimohama S, Tabaton M, Atwood CS, Petersen RB, Perry G, Smith MA: Neuroprotective properties of Bcl-w in Alzheimer disease. J Neurochem 2004, 89:1233–1240
8. Swerdlow RH, Khan SM: A "mitochondrial cascade hypothesis" for sporadic Alzheimer's disease. Med Hypotheses 2004, 63:8–20
9. Hirai K, Aliev G, Nunomura A, Fujioka H, Russell RL, Atwood CS, Johnson AB, Kress Y, Vinters HV, Tabaton M, Shimohama S, Cash AD, Siedlak SL, Harris PL, Jones PK, Petersen RB, Perry G, Smith MA: Mitochondrial abnormalities in Alzheimer's disease. J Neurosci 2001, 21:3017–3023
10. Trimmer PA, Swerdlow RH, Parks JK, Keeney P, Bennett JP Jr., Miller SW, Davis RE, Parker WD Jr.: Abnormal mitochondrial morphology in sporadic Parkinson's and Alzheimer's disease cybrid cell lines. Exp Neurol 2000, 162:37–50
11. Shin HW, Shinotsuka C, Torii S, Murakami K, Nakayama K: Identification and subcellular localization of a novel mammalian dynamin-related protein homologous to yeast Vps1p and Dnm1p. J Biochem 1997, 122:525–530
12. Imoto M, Tachibana I, Urrutia R: Identification and functional characterization of a novel human protein highly related to the yeast dynamin-like GTPase Vps1p. J Cell Sci 1998, 111:1341–1349
13. Kamimoto T, Nagai Y, Onogi H, Muro Y, Wakabayashi T, Hagiwara M: Dymple, a novel dynamin-like high molecular weight GTPase lacking a proline-rich carboxyl-terminal domain in mammalian cells. J Biol Chem 1998, 273:1044–1051
14. Zhu PP, Patterson A, Stadler J, Seeburg DP, Sheng M, Blackstone C: Intra- and intermolecular domain interactions of the C-terminal GTPase effector domain of the multimeric dynamin-like GTPase Drp1. J Biol Chem 2004, 279:35967–35974
15. Yoon Y, Pitts KR, Dahan S, McNiven MA: A novel dynamin-like protein associates with cytoplasmic vesicles and tubules of the endoplasmic reticulum in mammalian cells. J Cell Biol 1998, 140:779–793
16. McBride HM, Neuspiel M, Wasiak S: Mitochondria: more than just a powerhouse. Curr Biol 2006, 16:R551–R560
17. Smirnova E, Shurland DL, Ryazantsev SN, van der Bliek AM: A human dynamin-related protein controls the distribution of mitochondria. J Cell Biol 1998, 143:351–358
18. Li Z, Okamoto K, Hayashi Y, Sheng M: The importance of dendritic mitochondria in the morphogenesis and plasticity of spines and synapses. Cell 2004, 119:873–887
19. Nguyen PV, Marin L, Atwood HL: Synaptic physiology and mitochondrial function in crayfish tonic and phasic motor neurons. J Neurophysiol 1997, 78:281–294
20. Zuchner S, Mersiyanova IV, Muglia M, Bissar-Tadmouri N, Rochelle J, Dadali EL, Zappia M, Nelis E, Patitucci A, Senderek J, Parman Y, Evgrafov O, Jonghe PD, Takahashi Y, Tsuji S, Pericak-Vance MA, Quattrone A, Battaloglu E, Polyakov AV, Timmerman V, Schroder JM, Vance JM: Mutations in the mitochondrial GTPase mitofusin 2 cause Charcot-Marie-Tooth neuropathy type 2A. Nat Genet 2004, 36: 449–451
21. Kijima K, Numakura C, Izumino H, Umetsu K, Nezu A, Shiiki T, Ogawa M, Ishizaki Y, Kitamura T, Shozawa Y, Hayasaka K: Mitochondrial GTPase mitofusin 2 mutation in Charcot-Marie-Tooth neuropathy type 2A. Hum Genet 2005, 116:23–27
22. Delettre C, Lenaers G, Griffoin JM, Gigarel N, Lorenzo C, Belenguer P, Pelloquin L, Grosgeorge J, Turc-Carel C, Perret E, Astarie-Dequeker C, Lasquellec L, Arnaud B, Ducommun B, Kaplan J, Hamel CP: Nuclear gene OPA1, encoding a mitochondrial dynamin-related protein, is mutated in dominant optic atrophy. Nat Genet 2000, 26:207–210
23. Alexander C, Votruba M, Pesch UE, Thiselton DL, Mayer S, Moore A, Rodriguez M, Kellner U, Leo-Kottler B, Auburger G, Bhattacharya SS, Wissinger B: OPA1, encoding a dynamin-related GTPase, is mutated in autosomal dominant optic atrophy linked to chromosome 3q28. Nat Genet 2000, 26:211–215
24. Atamna H, Liu J, Ames BN: Heme deficiency selectively interrupts assembly of mitochondrial complex IV in human fibroblasts: relevance to aging. J Biol Chem 2001, 276:48410–48416
25. Begni B, Brighina L, Sirtori E, Fumagalli L, Andreoni S, Beretta S, Oster T, Malaplate-Armand C, Isella V, Appollonio I, Ferrarese C: Oxidative stress impairs glutamate uptake in fibroblasts from patients with Alzheimer's disease. Free Radic Biol Med 2004, 37:892–901
26. Gibson G, Martins R, Blass J, Gandy S: Altered oxidation and signal transduction systems in fibroblasts from Alzheimer patients. Life Sci 1996, 59:477–489
27. Sims NR, Finegan JM, Blass JP: Altered glucose metabolism in fibroblasts from patients with Alzheimer's disease. N Engl J Med 1985, 313:638–639
28. Cecchi C, Fiorillo C, Sorbi S, Latorraca S, Nacmias B, Bagnoli S, Nassi P, Liguri G: Oxidative stress and reduced antioxidant defenses in peripheral cells from familial Alzheimer's patients. Free Radic Biol Med 2002, 33:1372–1379
29. Huang HM, Fowler C, Xu H, Zhang H, Gibson GE: Mitochondrial function in fibroblasts with aging in culture and/or Alzheimer's disease. Neurobiol Aging 2005, 26:839–848
30. Atamna H, Killilea DW, Killilea AN, Ames BN: Heme deficiency may be a factor in the mitochondrial and neuronal decay of aging. Proc Natl Acad Sci USA 2002, 99:14807–14812
31. Uberti D, Lanni C, Carsana T, Francisconi S, Missale C, Racchi M, Govoni S, Memo M: Identification of a mutant-like conformation of p53 in fibroblasts from sporadic Alzheimer's disease patients. Neurobiol Aging 2006, 27:1193–1201
32. Kues WA, Carnwath JW, Paul D, Niemann H: Cell cycle synchronization of porcine fetal fibroblasts by serum deprivation initiates a non-conventional form of apoptosis. Cloning Stem Cells 2002, 4:231–243
33. Martelli F, Livingston DM: Regulation of endogenous E2F1 stability by the retinoblastoma family proteins. Proc Natl Acad Sci USA 1999, 96:2858–2863
34. Mallolas J, Esteve M, Rius E, Cabre E, Gassull MA: Antineutrophil antibodies associated with ulcerative colitis interact with the antigen(s) during the process of apoptosis. Gut 2000, 47:74–78
35. Zhu X, Lee HG, Casadesus G, Avila J, Drew K, Perry G, Smith MA: Oxidative imbalance in Alzheimer's disease. Mol Neurobiol 2005, 31:205–217
36. Naderi J, Lopez C, Pandey S: Chronically increased oxidative stress in fibroblasts from Alzheimer's disease patients causes early senescence and renders resistance to apoptosis by oxidative stress. Mech Ageing Dev 2006, 127:25–35
37. Askanas V, McFerrin J, Baque S, Alvarez RB, Sarkozi E, Engel WK: Transfer of beta-amyloid precursor protein gene using adenovirus vector causes mitochondrial abnormalities in cultured normal human muscle. Proc Natl Acad Sci USA 1996, 93:1314–1319
38. Devi L, Prabhu BM, Galati DF, Avadhani NG, Anandatheerthavarada HK: Accumulation of amyloid precursor protein in the mitochondrial import channels of human Alzheimer's disease brain is associated with mitochondrial dysfunction. J Neurosci 2006, 26:9057–9068
39. Manczak M, Anekonda TS, Henson E, Park BS, Quinn J, Reddy PH: Mitochondria are a direct site of A beta accumulation in Alzheimer's disease neurons: implications for free radical generation and oxidative damage in disease progression. Hum Mol Genet 2006, 15: 1437–1449
40. Lustbader JW, Cirilli M, Lin C, Xu HW, Takuma K, Wang N, Caspersen C, Chen X, Pollak S, Chaney M, Trinchese F, Liu S, Gunn-Moore F, Lue LF, Walker DG, Kuppusamy P, Zewier ZL, Arancio O, Stern D, Yan SS, Wu H: ABAD directly links Abeta to mitochondrial toxicity in Alzheimer's disease. Science 2004, 304:448–452

41. Frieden M, James D, Castelbou C, Danckaert A, Martinou JC, Demaurex N: Ca(2+) homeostasis during mitochondrial fragmentation and perinuclear clustering induced by hFis1. J Biol Chem 2004, 279:22704–22714
42. Exner N, Treske B, Paquet D, Holmstrom K, Schiesling C, Gispert S, Carballo-Carbajal I, Berg D, Hoepken HH, Gasser T, Kruger R, Winklhofer KF, Vogel F, Reichert AS, Auburger G, Kahle PJ, Schmid B, Haass C: Loss-of-function of human PINK1 results in mitochondrial pathology and can be rescued by parkin. J Neurosci 2007, 27:12413–12418
43. Poole AC, Thomas RE, Andrews LA, McBride HM, Whitworth AJ, Pallanck LJ: The PINK1/Parkin pathway regulates mitochondrial morphology. Proc Natl Acad Sci USA 2008, 105:1638–1643
44. Sheehan JP, Swerdlow RH, Miller SW, Davis RE, Parks JK, Parker WD, Tuttle JB: Calcium homeostasis and reactive oxygen species production in cells transformed by mitochondria from individuals with sporadic Alzheimer's disease. J Neurosci 1997, 17:4612–4622
45. Arnoult D: Mitochondrial fragmentation in apoptosis. Trends Cell Biol 2007, 17:6–12
46. Kelly BL, Vassar R, Ferreira A: Beta-amyloid-induced dynamin 1 depletion in hippocampal neurons: a potential mechanism for early cognitive decline in Alzheimer disease. J Biol Chem 2005, 280: 31746–31753
47. Atamna H, Boyle K: Amyloid-beta peptide binds with heme to form a peroxidase: relationship to the cytopathologies of Alzheimer's disease. Proc Natl Acad Sci USA 2006, 103:3381–3386
48. Atamna H, Frey WH 2nd: A role for heme in Alzheimer's disease: heme binds amyloid beta and has altered metabolism. Proc Natl Acad Sci USA 2004, 101:11153–11158
49. Frazier AE, Kiu C, Stojanovski D, Hoogenraad NJ, Ryan MT: Mitochondrial morphology and distribution in mammalian cells. Biol Chem 2006, 387:1551–1558
50. Uberti D, Carsana T, Bernardi E, Rodella L, Grigolato P, Lanni C, Racchi M, Govoni S, Memo M: Selective impairment of p53-mediated cell death in fibroblasts from sporadic Alzheimer's disease patients. J Cell Sci 2002, 115:3131–3138
51. Frank S, Gaume B, Bergmann-Leitner ES, Leitner WW, Robert EG, Catez F, Smith CL, Youle RJ: The role of dynamin-related protein 1, a mediator of mitochondrial fission, in apoptosis. Dev Cell 2001, 1:515–525
52. Lee YJ, Jeong SY, Karbowski M, Smith CL, Youle RJ: Roles of the mammalian mitochondrial fission and fusion mediators Fis1, Drp1, and Opa1 in apoptosis. Mol Biol Cell 2004, 15:5001–5011
53. Estaquier J, Arnoult D: Inhibiting Drp1-mediated mitochondrial fission selectively prevents the release of cytochrome c during apoptosis. Cell Death Differ 2007,
54. Westermann B: Merging mitochondria matters: cellular role and molecular machinery of mitochondrial fusion. EMBO Rep 2002, 3: 527–531
55. Zhu X, Raina AK, Perry G, Smith MA: Alzheimer's disease: the two-hit hypothesis. Lancet Neurol 2004, 3:219–226
56. Verstreken P, Ly CV, Venken KJ, Koh TW, Zhou Y, Bellen HJ: Synaptic mitochondria are critical for mobilization of reserve pool vesicles at Drosophila neuromuscular junctions. Neuron 2005, 47:365–378
57. Coleman P, Federoff H, Kurlan R: A focus on the synapse for neuroprotection in Alzheimer disease and other dementias. Neurology 2004, 63:1155–1162
58. Selkoe DJ: Alzheimer's disease is a synaptic failure. Science 2002, 298:789–791